Experimental Observation of Femtosecond Electron Beam Microbunching by Inverse Free-Electron-Laser Acceleration

Y. Liu,[1] X. J. Wang,[2] D. B. Cline,[1] M. Babzien,[2] J. M. Fang,[2] J. Gallardo,[2] K. Kusche,[2] I. Pogorelsky,[2] J. Skaritka,[2] and A. van Steenbergen[2]

[1]*University of California, Los Angeles, California 90095*

[2]*Brookhaven National Laboratory, Upton, New York 11973*

(Received 16 July 1997)

An electron beam microbunched on the optical wavelength scale of $\approx 2.5\ \mu$m by an inverse free electron laser accelerator was observed. The optimum bunching was achieved for a 1% energy modulation of a 32 MeV electron beam with 0.5 GW CO_2 laser power. The microbunching process was investigated by measuring the coherent transition radiation produced by the energy modulated electron beam. A quadratic dependence of the transition radiation signal on the electron beam charge was observed. The observed shortest wavelength of coherent transition radiation is less than 2.5 μm. The debunching process of the microbunched electron beam was experimentally investigated. [S0031-9007(98)06085-2]

PACS numbers: 29.27.Fh, 41.60.Cr, 41.75.Lx, 52.75.Va

Electron beams as short as a few hundred femtoseconds have been produced using a photocathode rf gun [1], thermionic rf gun [2], and magnetic bunch compressor [3] for coherent radiation generation, femtosecond x-ray production, and advanced accelerator applications. For laser accelerator applications, such as inverse Cerenkov accelerator [4], inverse free electron laser (IFEL) [5], and plasma laser accelerators [6], electron beam bunch lengths shorter than the laser wavelength or plasma wavelength are required for future high energy physics and other applications. That is, the electron beam must be microbunched on the order of a few femtoseconds, which is comparable to the optical wavelength. Microbunched electron beams play a fundamental role for the proposed UV and x-ray high gain harmonic generation (HGHG) free electron lasers (FEL) [7–9]. Microbunching of the electron beam is also critical for the successful operation of x-ray self-amplified spontaneous radiation FEL [10]. In this Letter, we report the experimental observation of electron beam microbunching on the optical wavelength ($<2.5\ \mu$m, 10 fs) using an inverse free electron laser accelerator [5] at the Brookhaven Accelerator Test Facility (ATF).

Using an IFEL to produce a microbunched electron beam has many advantages. The IFEL microbunching can be performed at a relative higher beam energy so emittance growth caused by the space-charge effect is negligible since it decreases rapidly with the electron beam energy. Furthermore, the IFEL microbunching takes place in vacuum, and no bending magnets and other medium are involved; there is little beam quality degradation during the microbunching. For laser accelerator applications, the same laser can be used both for IFEL microbunching and laser based accelerators [4,6]; IFEL microbunching provides natural synchronization between the laser for acceleration and the microbunched electron beam. The IFEL microbunching is basically the first part of HGHG FEL, the coherent harmonic radiation of the IFEL driving laser is generated by the microbunched electron beam in the second wiggler of the HGHG FEL. For UV and x-ray FELs, using microbunched electron beams will reduce the radiator wiggler length significantly.

The IFEL process is very similar to the FEL process; it couples the transverse motion of the electron beam with the electromagnetic wave in the presence of a periodic transverse wiggler magnetic field. In the FEL process, the electron beam is strongly bunched only in the exponential gain regime [11], which requires long wiggler and high-quality electron beam. The readily available high power lasers in the IR and visible wavelengths make IFEL as an optical wavelength microbuncher technically much less challenging, and economically more feasible.

Most techniques used for measuring the electron beam bunch length, such as streak camera and rf kicker cavity, are not suitable for optical wavelength microbunched electron beams because of their limited resolution. Transition radiation was used in our experiment to study the IFEL microbunching (debunching) process because of its promptness. The transition radiation from an electron beam can be described by [12]

$$\frac{d^2U}{d\omega d\Omega} = [N + N^2 F(\omega,\theta)] \frac{d^2u}{d\omega d\Omega}\bigg|_{\text{single}}, \quad (1)$$

where $\frac{d^2u}{d\omega d\Omega}|_{\text{single}}$ is the transition radiation intensity distribution for a single electron.

$$F(\omega,\theta) = \left| \int\int\int f(r,z) \exp(-i\vec{k}\cdot\vec{x}) d^3x \right|^2 \quad (2)$$

is a form factor, which is the Fourier transform of the electron beam distribution. It can be further divided into two parts; one is the so called longitudinal form factor, and the other is the transverse form factor. N is the number of electrons, ω is the radiation frequency, k is

 0031-9007/98/80(20)/4418(4)$15.00

TABLE I. The ATF beam parameters for IFEL microbunching experiment.

Injection energy	32 MeV
Electron beam bunch length	5 (psec, FWHM)
Normalize emittance (rms)	1.0 mm mrad
Charge	0.3 nC

the radiation wave number, θ is the radiation observation angle relative to electron beam, and Ω is the observational solid angle. Equation (1) shows that incoherent transition radiation is linearly proportional to the total number of electrons, while coherent transition radiation (TR) has a quadratic dependence on the number of electrons. Furthermore, Eq. (1) shows that the electron beam distribution is embedded into the coherent transition radiation, and significant coherent radiation is produced only if the electron beam bunch length is comparable to or less than the radiation wavelength observed.

An IFEL accelerator has been successfully operated at the ATF using a high power CO_2 laser [5]. The ATF accelerator system consists of a photocathode rf gun injector and two sections of SLAC-type traveling wave linac. It produces electron beams with an upper energy of 60 MeV; the beam parameters used for the microbunching experiment are listed in Table I. The electron beam produced by the photocathode rf gun was transported to the IFEL accelerator experiment through an electron beam transport line. The IFEL accelerator is located on the ATF beam line No. 2. The quadruple magnet doublet in front of the IFEL wiggler (Fig. 1) provides the electron beam optics matching for electron beam into the wiggler. Special beam profile monitors were installed before and after the wiggler; they are used for both e^- beam and CO_2 laser profile measurements. Nonintersective beam position monitors (BPM) were also placed both upstream and downstream from the IFEL wiggler. BPMs were used for both electron beam transmission studies through the IFEL wiggler and electron beam charge measurement. The microbunching diagnostics, which followed the downstream BPM, consists of a transition radiator inside a vacuum chamber, an optical transport system, a charge-coupled device (CCD) camera, and an infrared (IR) detector. The transition radiator is made up of a thin copper foil (2.5 mil), positioned perpendicular to the e^- beam and a 45° copper mirror behind it. The optical system consists of an IR lens positioned right outside the ZnSe window of the vacuum chamber, a gold coated parabolic copper mirror which focuses the IR light onto the IR detector, and a HeNe laser used for optical alignment. The CCD camera can replace the IR lens for electron beam profile and position measurements using transition radiation generated on the copper foil. The IR detector is a liquid nitrogen cooled indium antimonide (InSb) detector which is sensitive to radiation wavelengths ranging from 1.0 to 5.5 μm; the sensitive area is 1×1 mm^2. The IR detector is located 60 cm away from the radiator chamber and is well shielded by lead blocks. All components including the radiator vacuum chamber were mounted on a longitudinal translation stage driven by a remote-controlled stepping motor. This allows the microbunching diagnostic system to travel along the e^- beam path, and studying the debunching process of the microbunched electron beam. The maximum travel distance of the translation stage is 40 cm.

The IFEL wiggler [5] is a pulsed electromagnetic wiggler with a period of 3.0 cm and a peak magnetic field of 1 T. The CO_2 laser pulse was injected into the electron beam pipe through a ZnSe window on the dipole magnet vacuum chamber. The CO_2 laser pulse was transported into the wiggler through a 2.8 mm (I.D.) circular low-loss sapphire waveguide.

The ATF IFEL accelerator was optimized for the interaction between the CO_2 laser and electron beam [5]. The electron beam interacts with the CO_2 laser pulse over all phases of the light wave since the electron beam bunch length (10 ps, 3 mm) is much longer than the CO_2 wavelength (10.6 μm). Consequently, half of the electrons are accelerated and the other half are decelerated. That is, the IFEL introduces energy modulation in the electron beam. After a certain drift distance, faster electrons will catch up

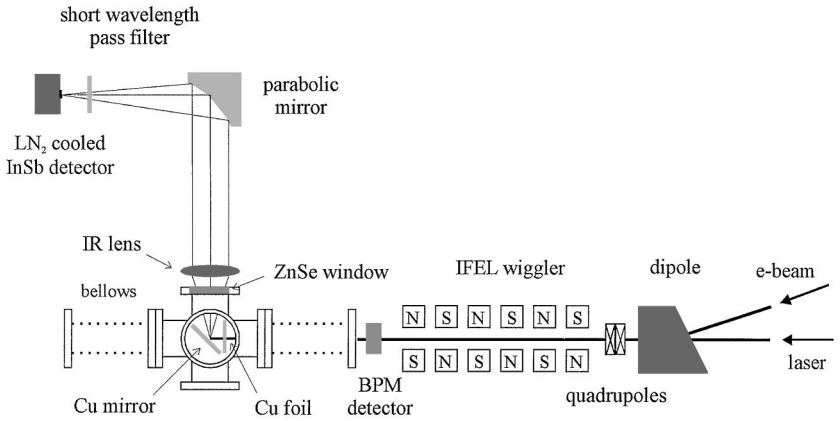

FIG. 1. Schematic of the microbunching experimental setup for the IFEL accelerator. The IFEL wiggler is 0.5 m long; the schematic is not drawn to scale.

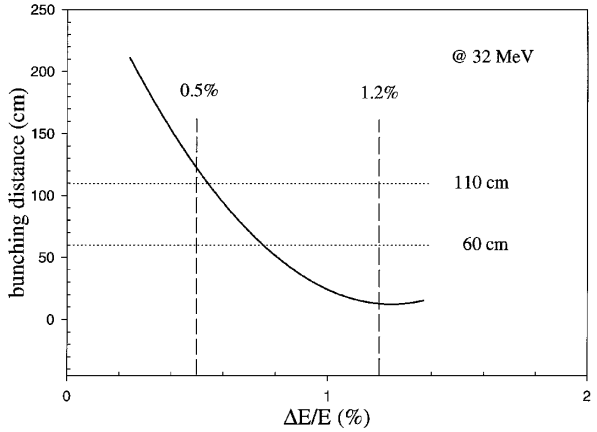

FIG. 2. The optimum bunching position as a function of the energy modulation calculated by 1D simulation.

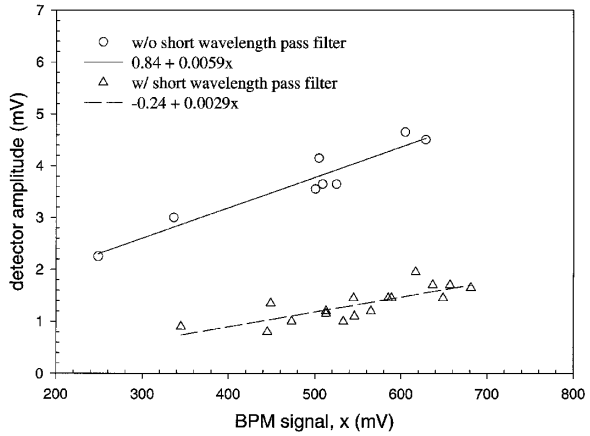

FIG. 3. The IR detector noise measurements with simultaneous presence of the wiggler, the e^- beam, and the CO_2 laser beam. The circles represent the noise taken without a short wavelength pass filter. The uptriangle is with the 2.5 μm filter. The BPM signal is proportional to the total charge (eN) of the electron beam.

with those slower ones resulting in a longitudinal density modulation (bunching). The optimum bunching is defined in such a way that the longitudinal phase space of electron beam rotates 90°, so the energy modulation is fully converted into spatial modulation. The bunching distance in our experiment is measured from the exit of the IFEL wiggler, while the debunching distance starts where the optimum bunching occurred.

A 1D IFEL computer simulation code was used to predict the optimum bunching distance as a function of e^- beam energy modulation (Fig. 2). Figure 2 shows that an energy modulation from $\pm 0.5\%$ to $\pm 1.2\%$ for a 32 MeV e^- beam will allow the optimum bunching to fall into the traveling range of the microbunch detector.

The electron beam energy for microbunch experiment was set as low as possible (32 MeV) within the IFEL resonance for the following reasons. The IFEL wiggler is a planar type wiggler; it provides only vertical focusing for the electron beam, and the strength of the wiggler focusing for normal IFEL operation is almost a factor of 2 stronger than that of the quadrupole doublet in front of the wiggler. By lowering the beam energy, we can reduce the wiggler strength, and thus achieve better control of the transverse beam profile at the CTR target without introducing space-charge effect. Initially, a CCD camera replacing the IR lens near the radiator chamber was used for electron beam profiles optimization by observing the optical transition radiation.

The electron beam energy modulation by the IFEL was measured using a spectrometer located at the end of the beam line. By adjusting the CO_2 laser power we were able to tune the energy modulation of the electron beam to about 1% which placed the optimum bunching at the upstream of the translation stage (Fig. 2).

We have carried out systematic experimental studies of the noise detected by the IR detector. One of the noise sources is the x ray induced by the e^- beam, and the other is broadband IR radiation produced by the CO_2 laser as the high power CO_2 laser beam propagates through the sapphire waveguide. The x-ray noise level was reduced to less than 1 mV by using lead to shield the IR detector. The IR noise was substantially suppressed when we adopted the foil plus mirror transition radiator configuration. The copper foil of the radiator is positioned perpendicular to the electron beam; it prevents the IR noise and the CO_2 laser beam from reaching the IR detector. Figure 3 shows the noise observed by the IR detector after the shielding was implemented. The noise measurements were taken with the simultaneous presence of the wiggler magnetic field, the e^- beam, and the CO_2 laser. To avoid the IFEL interaction, the relative timing between the e^- beam and the CO_2 laser was adjusted in order to ensure no temporal overlapping between them. Two sets of noise measurement were taken. Higher noise level was observed without any filter. The other one was taken with a 2.5 μm short-wavelength pass filter. The linear dependence of the noise on the beam intensity is mainly due to incoherent transition radiation generated by the e^- beam.

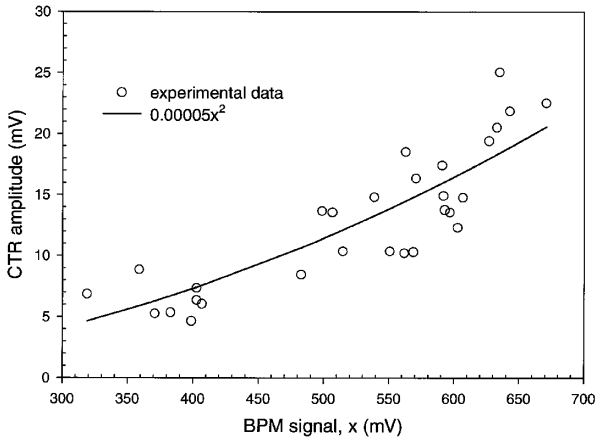

FIG. 4. The transition radiation signal as a function of the total number of electrons. The BPM signal is proportional to the total charge (eN) of the electron beam.

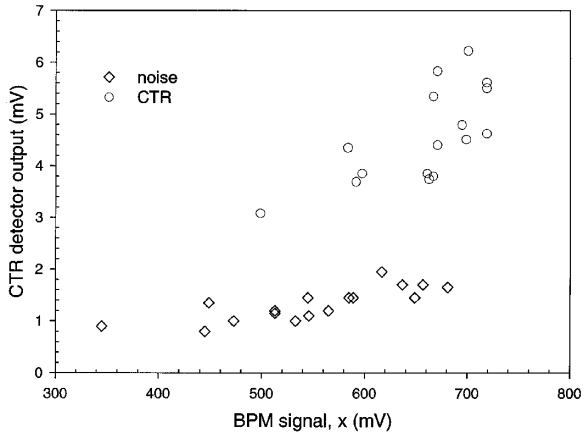

FIG. 5. The coherent transition radiation detected by InSb IR detector with shorter wavelength pass filter. The x axis is the BPM signal which is proportional to the charge.

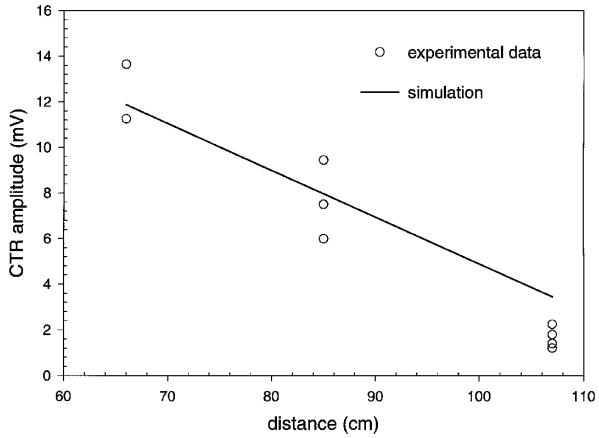

FIG. 6. The comparison of 1D simulation and experimental measurement of CTR signal changes as a function of the debunching distance. The circles are the experimental data and the solid line is the simulation result.

After the electron beam profile on the radiator and the electron energy modulation were optimized, the microbunching process was studied by measuring the transition radiation generated by the energy modulated electron beam. Figure 4 shows the transition radiation detected by the IR detector as a function of the beam charge without any filter. The charge of the electron beam was measured by the BPM located after the wiggler. Both linear (ax) and quadratic (bx^2) least squares fits of the data were performed. The r^2 of the fitting for linear fit and quadratic fit are 0.324 and 0.732, respectively. Comparing with the noise measurement data presented in Fig. 3, in which transition radiation from unbunched electron beam was included, we conclude that the transition radiation intensity has a quadratic dependence on the beam charge. This confirms that the transition radiation is coherent and the coherent radiation wavelength is shorter than the InSb IR detector long wavelength limit 5.5 μm. The fluctuation of the CTR signal can be attributed to the shot-by-shot power fluctuation in the CO_2 laser.

Furthermore, a short wavelength pass filter with a 2.5 μm cutoff wavelength was placed in front of the InSb IR detector; the coherent transition radiation was still observable and well above the noise level (Fig. 5). The reduction of CTR signal shown in Fig. 5 comparing with Fig. 4 is due to the following causes. The presence of the 2.5 μm filter cuts the InSb IR detector bandwidth in half, and its transmission rate is about 85%. The efficiency of InSb IR detector drops to less than 50% for a wavelength shorter than 2.5 μm. Considering those factors, we conclude that the microbunch length is much shorter than 5 μm and close to the fourth harmonic (2.5 μm) of the CO_2 laser.

The microbunch process as a function of the debunching distance was also studied. For 1% energy modulation, the optimum microbunching occurred at about 25 cm from the wiggler exit. This position allows us to take advantage of the full travel distance of the translation stage to study the debunching process. The debunching process was investigated by measuring the CTR signal amplitude variation as the radiator is moved down along the electron beam line to different positions. The CTR signal amplitude decreased as the radiator moved away from the optimum bunching position (Fig. 6). This implies that the bunch length increases with the drift distance. Figure 6 shows the agreement between the 1D simulation and the experimental results. The CO_2 laser energy and the e^- beam charge fluctuations are about $\pm 20\%$ and $\pm 5\%$, respectively, during the measurement.

We have experimentally demonstrated the IFEL microbunching process by measuring the coherent transition radiation signal and its variation as a function of the debunching distance. Using the filter cutoff wavelength as the reference, we conclude that the microbunch length is a fraction of the CO_2 wavelength ($\sim$2.5 μm).

We are grateful for the support provided by the ATF staff, Dr. I. Ben-Zvi for his encouragement, and B. Cahill, B. Harrington, R. Malone, and M. Montemagno for their technical support. We acknowledge helpful discussions with Dr. J. Rosenzweig and E. B. Blum. This work is supported by U.S. Department of Energy.

[1] X. J. Wang *et al.,* Phys. Rev. E **54**, R3121 (1996).
[2] H. C. Lihn *et al.,* Phys. Rev. E **53**, 6413 (1996).
[3] B. E. Carlsten *et al.,* Phys. Rev. E **53**, R2072 (1996).
[4] W. D. Kimura *et al.,* Phys. Rev. Lett. **74**, 546 (1995).
[5] A. van Steenbergen *et al.,* Phys. Rev. Lett. **77**, 2690 (1996).
[6] K. Nakajima *et al.,* Phys. Rev. Lett. **74**, 4428 (1995).
[7] I. Ben-Zvi *et al.,* Nucl. Instrum. Methods Phys. Res., Sect. A **318**, 208 (1992).
[8] L. H. Yu, Phys. Rev. A **44**, 5178 (1991).
[9] V. V. Goloviznin *et al.,* Phys. Rev. E **55**, 6002 (1997).
[10] R. Bonifacio *et al.,* Opt. Commun. **50**, 373 (1984).
[11] N. M. Kroll *et al.,* IEEE J. Quantum Electron. **17**, 1436 (1981); **A365**, 255 (1995).
[12] Y. Shibata *et al.,* Phys. Rev. A **45**, R8340 (1992).